PROCEEDINGS OF SCIENCE

Information field based global Bayesian inference of jet transport coefficient and dijet grandient tomography of heavy-ion collisions

Yayun He,[a,b] **Xin-Nian Wang**[c,*] **and Man Xie**[a,b]

[a] *Guangdong Provincial Key Laboratory of Nuclear Science, Institute of Quantum Matter, South China Normal University, Guangzhou 510006, China*

[b] *Guangdong-Hong Kong Joint Laboratory of Quantum Matter, Southern Nuclear Science Computing Center, South China Normal University, Guangzhou 510006, China*

[c] *Nuclear Science Division MS 70R0319, Lawrence Berkeley National Laboratory, Berkeley, California 94720, USA*

E-mail: xnwang@lbl.gov

In this talk, two recent developments in jet tomography of heavy-ion collisions are discussed: (1) An information field approach to modeling the prior function distributions that is free of long-range correlations is applied to the first global Bayesian inference of the jet transport coefficient $\hat{q}$ as a function of temperature (T) using global experimental data on single hadron, dihadron and γ-hadron spectra. The extracted $\hat{q}/T^3$ exhibits a strong T-dependence as a result of the progressive constraining power when data from more central collisions and at higher colliding energies are incrementally included. (2) Gradient jet tomography is extended to dijets in heavy-ion collisions. With fixed momentum of the leading jet, the transverse asymmetry of energetic hadrons from the subleading jet are shown to provide reasonable estimate of the dijet initial production points. This can be used to study geometric dependence of other jet observables such as jet-induced medium response.

HardProbes2023
26-31 March 2023
Aschaffenburg, Germany

*Speaker

PoS(HardProbes2023)164

1. Introduction: Parton energy loss and jet quenching at RHIC and LHC can provide unprecedented opportunities to explore properties of quark-gluon plasma (QGP) in high-energy heavy-ion collisions. One of these properties, jet transport coefficient $\hat{q}$ or the transverse momentum broadening squared per unit distance due to jet-medium interaction, have been extracted from the combined data on the suppression of single inclusive hadron spectra at both RHIC and LHC by the JET Collaboration [1] and similar efforts. Such extraction of QGP properties rely on jet tomographic study of heavy-ion collisions and Bayesian statistic inference technique. In the current extraction of the jet transport coefficient, one assumes the spatial distribution of the initial jet production points according to the Glauber model with the Woods-Saxon nuclear distribution and the space-time evolution of the QGP matter from a relativistic hydrodynamic model. Though the azimuthal anisotropy of jet quenching [2, 3] can shed light on the averaged path-length dependence of jet transport, the study of jet quenching with a localized initial jet production position can provide more direct information about the space-time profile of the jet transport coefficient. The Bayesian inference technique relies on the Bayes' Theorem: "Posterior = Prior × Likelihood". It describes how a prior belief of the distribution of some physical parameters is updated to the posterior distribution according to comparisons between theory and experimental data, as encoded in the likelihood function that quantifies the model's descriptive power. All recent Bayesian inference of the jet transport coefficient rely on a parameterized form of temperature and momentum dependence and the experimental data are limited to single inclusive hadron or jet spectra.

We will discuss two recent new developments in the jet tomography: (1) An information field approach to modeling the prior function distributions that is free of long-range correlations is applied to the first global Bayesian inference of the jet transport coefficient $\hat{q}$ as a function of temperature (T) [4]. The extracted $\hat{q}/T^3$ exhibits a strong T-dependence as a result of the progressive constraining power when data from more central collisions and at higher colliding energies are incrementally included. (2) Gradient jet tomography is extended to dijets in heavy-ion collisions. With fixed momentum of the leading jet, the transverse asymmetry of energetic hadrons from the subleading jet are shown to provide reasonable estimate of the dijet initial production points. This can be used to study geometric dependence of other jet observables such as jet-induced medium response.

2. IF-based Bayesian inference of $\hat{q}$: Energy loss of quarks and gluons inside QGP can lead to the suppression of large transverse momentum ($p_{\rm T}$) jets and hadrons in high-energy heavy-ion (A+A) collisions [5, 6]. Parton energy loss [7],

$$\frac{dE}{dL} = \frac{\alpha_s N_c}{4}\hat{q}L, \tag{1}$$

is controlled on the other hand by the jet transport coefficient $\hat{q}$, defined as the transverse momentum broadening squared per unit length [7]. It can depend on both the local temperature along the jet trajectory inside QGP and parton initial energy. We use the next-leading-order (NLO) parton model [8] to calculate single inclusive hadron, di-hadron and γ-hadron spectra in proton-proton (p+p) and A+A collisions, which are factorized into parton distribution functions (PDF) of the proton or nuclei, partonic scattering cross sections, and parton fragmentation functions (FF). In heavy-ion collisions, medium-modified FF's are assumed to be given by the vacuum ones with reduced parton energy due to energy loss plus fragmentation of radiated gluons [9].

The radiative energy loss of a parton with energy E within the higher-twist approach [10] is,

$$\frac{\Delta E_a}{E} = \frac{2C_A\alpha_s(E^2)}{\pi}\int_{\tau_0}^{\infty}d\tau\int\frac{dl_{\rm T}^2}{l_{\rm T}^2(l_{\rm T}^2+\mu_D^2)}\int dz\left[1+(1-z)^2\right]\hat{q}_a(T(\tau))\sin^2\frac{l_{\rm T}^2(\tau-\tau_0)}{4z(1-z)E}, \quad (2)$$

where $C_A = 3$, $\alpha_s(E^2)$ the strong running-coupling constant, $l_{\rm T}$ the transverse momentum and z the longitudinal momentum fraction of the radiated gluon. The Debye screening mass squared is $\mu_D^2 = (1+n_f/6)g^2T^2 = (1+n_f/6)4\pi\alpha_s T^2$, for $n_f = 3$ quark flavors and strong coupling constant is set to $\alpha_s = 0.3$. The integral in time is along the jet path starting at time $\tau_0 = 0.6$ fm/c. The jet transport coefficient of a gluon $\hat{q}_A$ is 9/4 times that of a quark $\hat{q}_F$. It is assumed to depend on the local temperature T and negligible in the hadron phase below $T_c = 165$ MeV. The space-time profiles of T and the four-velocity of the QGP fluid are given by the CLVisc 3+1 D hydrodynamic simulations [11] with initial conditions given by the TRENTo model [12] averaged over 200 events for each centrality bin. An overall envelope function in the spatial rapidity is used to generalize the TRENTo initial condition at middle rapidity to a 3D distribution. Parameters in the initial condition and the QGP transport coefficients are fitted to data on bulk hadron production. Uncertainties on the inferred $\hat{q}$ due to variations of these medium-related parameters are not the focus of this work and are not considered.

The IF approach considers the unconditioned function as a random field, normally assumed as a Gaussian random field (F) specified by a mean and a covariance function,

$$\langle F(x)\rangle = \mu(x), \quad \langle \delta F(x)\delta F(x')\rangle = C(x,x'), \quad (3)$$

where $\delta F(x) = F(x) - \mu(x)$ and higher cumulants vanish. We use the scaled quantity $F(x) = \ln(\hat{q}/T^3)$ as a random field in variable $x = \ln(T/\text{GeV})$, which guarantees the positivity of $\hat{q}/T^3$. We also assume a prior that has $\mu =$ const and the correlation function takes the Gaussian form,

$$C(x,x') = \sigma^2\exp\left[-(x-x')^2/2l^2\right], \quad (4)$$

where σ controls the variation of the random function with respect to the mean and l is correlation length. The functional values at inputs x and x' are decorrelated from each other for $|x-x'| \gg l$, which means that the high-temperature prior is unaffected by data that are only sensitive to $\hat{q}(T)$ at low temperature. This is the key to overcoming the problem of unnecessary long-range correlations in the explicit parameterizations.

In this study, we fix $\mu = 1.36$, $\sigma = 0.7$ and $l = \ln(2)$ for the Gaussian random field F and perform an exponential transformation $\hat{q}/T^3 = \exp(F)$. Fig. 1(left)(a) shows 100 random samples of $\hat{q}/T^3$ from the IF priors. The 95% credible interval (CI) of the prior covers most of the range $0.8 \lesssim \hat{q}/T^3 \lesssim 15$ from past analyses, as shown (gray band) in Fig. 1(left)(b). Two sets of conditional random functions, "High-T var." prior constrained to $\hat{q}/T^3 = 4\pm0.1$ at $0.15 < T < 0.2$ GeV but are allowed to vary in the high temperature region and "Low-T var." prior restricted to $\hat{q}/T^3 = 4\pm0.1$ at $0.3 < T < 0.4$ GeV and can vary at low temperatures almost in the full range of prior values of $\hat{q}/T^3$ as shown in Fig. 1(left)(b). It is clear that the prior at high T and low T are indeed uncorrelated.

Using model emulators and all existing experimental data on $R_{\rm AA}^h$, $I_{\rm AA}^{hh}$ and $I_{\rm AA}^{\gamma h}$ at both RHIC and LHC energies with total 243 experimental data points [4], we have carried out the Bayesian

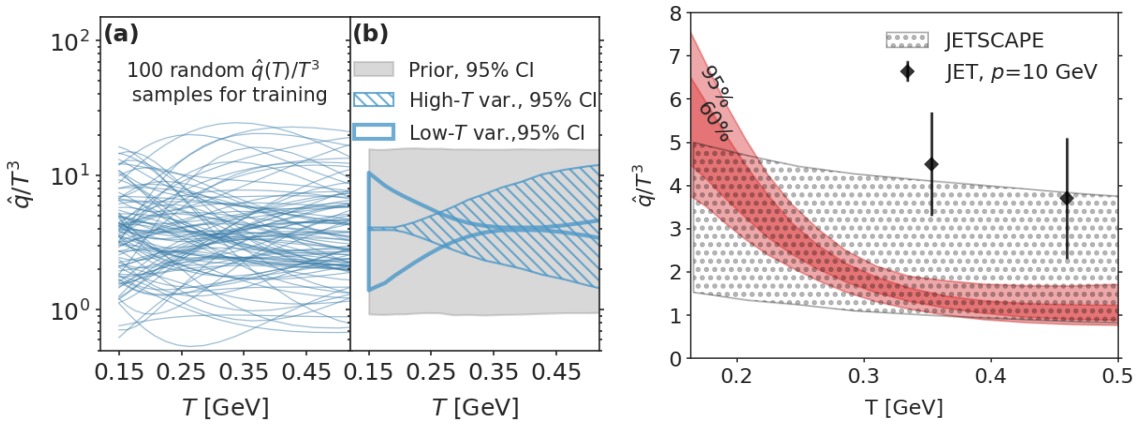

Figure 1: (left)(a) 100 prior random functions for $\hat{q}/T^3$ from the IF approach. (left)(b) Prior random functions for $\hat{q}/T^3$ at 95% CI that are restricted to $\hat{q}/T^3 = 4 \pm 0.1$ at $0.15 < T < 0.2$ GeV (High-T var., hatched) or $0.3 < T < 0.4$ GeV (Low-T var., unhatched) as compared to unconditioned prior (grey). (right)Posterior $\hat{q}/T^3$ from the global IF-based Bayesian analysis (red) as compared to results from JET Collaboration (symbols) [1] and JETSCAPE (dot-hatched) [13].

inference of $\hat{q}(T)$. Shown in Fig. 1(right) is the final posterior $\hat{q}/T^3$ (red band) in 95% CI as compared to the fit by the JET Collaboration [1] (symbols) and the JETSCAPE (95% CI, line-hatched) [13] and LIDO (95% CI, dot-hatched) [14] Bayesian analyses. The blue lines within the band are 20 random posterior samples to illustrate the distribution and correlation of the posterior $\hat{q}/T^3$. The extracted $\hat{q}/T^3$ is consistent with the JETSCAPE result [13] at 95% CI except at temperatures close to T_c where a stronger temperature dependence arises from the combined constraints by experimental data in central and peripheral collisions at different colliding energies.

3. Dijet gredient tomography: Since the jet transport coefficient $\hat{q}$ characterizes the transverse momentum broadening, it determines the diffusion of a propagating jet parton in both the transverse momentum and coordinate. If the spatial distribution of $\hat{q}$ is not uniform, its transverse gradient will lead to a drift in the final parton's transverse momentum and spatial distribution, causing asymmetries in its final distributions [15, 16]. One can define a transverse momentum asymmetry to characterize this drift which will depend on the propagation length and transverse gradient of $\hat{q}$. Given the geometry of the QGP medium and its time evolution, one can in return use this transverse momentum asymmetry to localize the initial production points of the selected jets in the transverse plane. Such a gradient jet tomography has been demonstrated for γ jets in heavy-ion collisions [17]. We will also apply this gradient tomography to dijets in heavy-ion collisions here.

Under the assumption that the transverse momentum is small $k_\perp/E \ll 1$ for a parton with energy E, Boltzmann transport equation for the parton can be cast into a drift-diffusion equation in the transverse direction,

$$\frac{\partial f}{\partial t} + \frac{\vec{k}_\perp}{E} \cdot \frac{\partial f_a}{\partial \vec{r}_\perp} = \frac{\hat{q}}{4} \vec{\nabla}^2_{k_\perp} f(\vec{k}_\perp, \vec{r}_\perp). \tag{5}$$

For a jet transport coefficient with small linear dependence in the transverse direction, $\hat{q} = \hat{q}_0 + \vec{x}_\perp \cdot \vec{a}$,

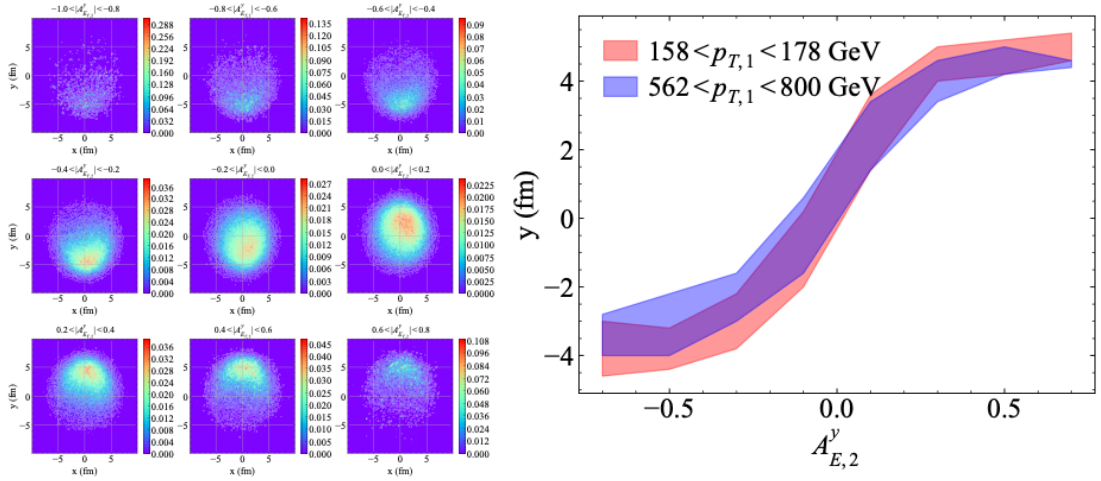

Figure 2: (left)Transverse distributions of the initial dijet production points for different values of the transverse asymmetry A_E^y.(right) Averaged vaule of the transverse position y of the initial dijet production points as a function of the transverse asymmetry A_E^y.

one can find the solution for the momentum distribution,

$$f(\vec{k}) = f^{(0)}(\vec{k}) - \frac{\vec{a}\cdot\vec{k}_\perp}{3\hat{q}_0 E} t \left(1 - \frac{k_\perp^2}{2\hat{q}_0 t}\right) f^{(0)}(k_\perp) + O(a^2), \tag{6}$$

with the initial condition $f(\vec{k}_\perp, t=0) = (2\pi)^2\delta^2(\vec{k}_\perp)$, which indeed develops an asymmetry in the transverse momentum distribution, where $f^{(0)}(k_\perp) = (4\pi/\hat{q}_0 t)\exp(-k_\perp^2/\hat{q}_0 t)$

Using the approximate back-to-back configuration of dijet, one can select the direction of the leading jet to coincide with the reaction plane. We define a momentum asymmetry for partons from the sub-leading jet relative to the plane $\vec{n}$ defined by the beam and the leading jet,

$$A_E^{\vec{n}} = \frac{\int d^3r d^3k \omega f_a(\vec{k},\vec{r})\mathrm{Sign}(\vec{k}\cdot\vec{n})}{\int d^3r d^3k \omega f_a(\vec{k},\vec{r})}. \tag{7}$$

The sign and value of the momentum asymmetry will depend on the jet propagation length and the local gradient of $\hat{q}$ perpendicular to the propagation path which ultimately depend on the initial position and direction of the jet production. We have used linear Boltzmann transport (LBT) model to simulate dijet production and propagation in heavy-ion collisions. The LBT model includes both $2 \to 2$ elastic parton scattering and inelastic processes of medium induced $2 \to 2+n$ multiple gluon radiation for both jet shower and medium recoil partons according to the Boltzmann equation [18, 19]. The CLVisc hydrodynamic model [11] is used to provide the space-time profile of the local temperature and fluid velocity in the QGP medium.

Shown in Fig. 2 (left) are the distribution of the initial dijet production points for different values of the asymmetry A_E^y for partons with $p_T > 3$ GeV/c from the subleading jet from LBT simulations of central 0-10% Pb+Pb collisions at $\sqrt{s} = 5.02$ TeV. Fig. 2 (right) shows the averaged value of the transverse position (y) as a function of the transverse asymmetry. For positive (negative) values of $A_{E_\perp}^y$, the initial dijet production position is distributed around a region above (below) and away from the center of the overlapped nuclei. By selecting the value of the transverse asymmetry,

one can therefore localize the transverse position of the initial jet production position for a more detailed study of jet quenching and the properties of the QGP matter.

Acknowledgement: Some work here is done in collaboration with W. Ke and H. Zhang. This work is supported by NSFC under Grant Nos. 11935007, 11861131009, 11890714, 12075098 and 12147134, by Guangdong Major Project of Basic and Applied Basic Research No. 2020B0301030008, by Guangdong Basic and Applied Basic Research Foundation No. 2021A1515110817, by Science and Technology Program of Guangzhou No.2019050001, by U.S. DOE under Contract No. DE-AC02-05CH11231, by US NSF under Grant OAC-2004571 within the X-SCAPE Collaboration, and by the LDRD Program at LANL. Computations are performed at NSC3 and NERSC.

References

[1] K. M. Burke *et al.* [JET], Phys. Rev. C **90**, no.1, 014909 (2014).

[2] X. N. Wang, Phys. Rev. C **63**, 054902 (2001).

[3] M. Gyulassy, I. Vitev and X. N. Wang, Phys. Rev. Lett. **86**, 2537-2540 (2001).

[4] M. Xie, W. Ke, H. Zhang and X. N. Wang, [arXiv:2206.01340 [hep-ph]].

[5] M. Gyulassy and M. Plumer, Phys. Lett. B **243**, 432-438 (1990).

[6] X. N. Wang and M. Gyulassy, Phys. Rev. Lett. **68**, 1480-1483 (1992) doi:10.1103/PhysRevLett.68.1480

[7] R. Baier, Y. L. Dokshitzer, A. H. Mueller, S. Peigne and D. Schiff, Nucl. Phys. B **483**, 291-320 (1997).

[8] J. F. Owens, Rev. Mod. Phys. **59**, 465 (1987) doi:10.1103/RevModPhys.59.465

[9] H. Zhang, J. F. Owens, E. Wang and X. N. Wang, Phys. Rev. Lett. **98**, 212301 (2007).

[10] X. N. Wang and X. F. Guo, Nucl. Phys. A **696**, 788-832 (2001).

[11] L. G. Pang, H. Petersen and X. N. Wang, Phys. Rev. C **97**, no.6, 064918 (2018).

[12] J. S. Moreland, J. E. Bernhard and S. A. Bass, Phys. Rev. C **92**, no.1, 011901 (2015).

[13] S. Cao *et al.* [JETSCAPE], Phys. Rev. C **104**, no.2, 024905 (2021).

[14] W. Ke and X. N. Wang, JHEP **05**, 041 (2021).

[15] Y. Fu, J. Casalderrey-Solana and X. N. Wang, Phys. Rev. D **107**, no.5, 054038 (2023).

[16] J. Barata, A. V. Sadofyev and X. N. Wang, Phys. Rev. D **107**, no.5, L051503 (2023).

[17] Y. He, L. G. Pang and X. N. Wang, Phys. Rev. Lett. **125**, no.12, 122301 (2020).

[18] Y. He, T. Luo, X. N. Wang and Y. Zhu, Phys. Rev. C **91**, 054908 (2015) [erratum: Phys. Rev. C **97**, no.1, 019902 (2018)].

[19] T. Luo, Y. He, S. Cao and X. N. Wang, [arXiv:2306.13742 [nucl-th]].